

A Sub-Arcsecond Pointing Stability Fine Stage for a High Altitude Balloon Platform

Laura Jones-Wilson, Sara Susca,
Christina Diaz, Herrick Chang,
Elizabeth Duffy, Robert
Effinger, Derek Lewis, Kurt
Liewer, Kevin Lo, Hared Ochoa,
Joseph Perez, Aadil Rizvi, Carl
Seubert, and Carson Umsted
Jet Propulsion Laboratory,
California Institute of
Technology
4800 Oak Grove Dr.
Pasadena, CA 91109
laura.l.jones@jpl.nasa.gov,
sara.susca@jpl.nasa.gov,
christina.diaz@jpl.nasa.gov

Michael Borden
Author was with:
Jet Propulsion
Laboratory, California
Institute of Technology
4800 Oak Grove Dr.
Pasadena, CA 91109

Author is now with:
General Atomics ASI
16868 Via Del Campo
Court, San Diego, CA
92127

Paul Clark, Richard Massey
Centre for Advanced
Instrumentation,
Durham University,
Department of Physics
South Road,
Durham
DH1 3LE,
United Kingdom

Michael Porter
Author was with:
Jet Propulsion
Laboratory, California
Institute of Technology
4800 Oak Grove Dr.
Pasadena, CA 91109

Author is now with:
California Institute of
Technology
1216 E. California
Blvd., MS 11-17
Pasadena, CA 91125

Abstract—High-altitude balloons (HABs) are platforms for collecting astrophysical and planetary science data that offer a number of advantages compared to conventional ground-based or space-based systems. However, they also pose a set of new environmental challenges that must be addressed in order to offer a viable alternative to ground- or space-based assets. In particular, maintaining science-quality pointing stability is a critical challenge for HAB platforms. For these missions, dynamic errors must be limited to a fraction of the observation wavelength, so as the wavelength becomes smaller, it becomes more difficult to meet the needed performance. As a result, there are very few existing pointing stabilization solutions that use visible-spectrum guide stars, despite their relatively wide distribution across the sky. This paper describes the results achieved with the STABLE (Sub-arcsecond Telescope And BaLloon Experiment) project whose goal is to provide the fine pointing stage for a balloon-borne platform observing in the visible wavelength.

TABLE OF CONTENTS

1. INTRODUCTION	1
2. RELEVANT PREVIOUS HAB MISSIONS	2
3. MISSION OVERVIEW	3
4. THE BALLOON ENVIRONMENT AND ITS CHALLENGES	4
5. STABLE DESIGN	5
6. POINTING ERROR BUDGET	10
7. STABLE PERFORMANCE	12
8. SUMMARY	13
ACKNOWLEDGEMENTS	14
REFERENCES	15
BIOGRAPHY	15

1. INTRODUCTION

High-altitude balloons (HABs) are an increasingly popular platform for astronomical and planetary science observations because they can provide access to space-like seeing (even in spectral bands absorbed by the atmosphere) at lower costs than most space-based observatories. In order to support science missions, HAB observatories require the ability to point to arbitrary parts of the sky and maintain the attitude within a stability bound driven by the specific observation being performed. This stability bound requirement often depends on the observing wavelength: the shorter the wavelength, the more stable the platform has to be. Thus, visible or ultraviolet observatories often have the most stringent pointing performance requirements, where many applications necessitate sub-arcsecond-level pointing stability over the integration period, which can be on the order of hours. Although some platforms have demonstrated this level of stability on an HAB using bright or extended guide sources, these limitations on the guide target similarly limit the science available from that platform. Surveys in particular are often unable to use bright guide stars exclusively because these stars are not distributed evenly in the sky. No solution has yet been demonstrated to achieve very fine pointing stability when using more widely distributed (but relatively dim) visible stellar targets. This work documents a HAB pointing payload designed to do exactly that.

BIT-STABLE (Balloon-borne Imaging Testbed, Sub-arcsecond Telescope And BaLloon Experiment) is a joint experiment and technology demonstration with NASA's Jet Propulsion Laboratory (JPL), the University of Toronto, University of Durham, and University of Edinburgh, that seeks to demonstrate sub-arcsecond-class pointing stability on an HAB using relatively dim guide

stars in the visible spectrum. The system uses a two-stage pointing architecture, where the coarse stage (BIT) [1] provides three-axis pointing control to stellar targets and coarse pointing stability to the fine stage (STABLE). STABLE, the main focus of this paper, is designed to meet its level-1 requirements, which are to achieve 100 milliarcsecond pointing stability over 60 seconds when guiding from a point-source target with a signal-to-noise ratio on the STABLE detector of 25. The system must achieve this performance from a HAB using measurements in the 400 nm to 900 nm spectral band. In order to accomplish these objectives, STABLE consists of a 0.5 m optical Ritchey-Chrétien telescope with an integrated optical bench assembly attached behind the primary mirror. This assembly houses a control system that includes a guide camera, an attitude rate sensor, and a fast steering mirror actuator, along with other support subsystems.

Although STABLE has not yet flown, relevant analysis and laboratory testing indicates that its target pointing performance can be met under most of its expected flight conditions. This paper first describes the pointing stability performance on other platforms for context and then provides some background on the BIT-STABLE concept of operations. Then, it explains the high-level STABLE error budgets developed to support the overall pointing stability objective, and explains how the STABLE hardware and software design supports the assessments in the budgets. Finally, the paper summarizes the analytical and experimental pointing results and explains their implications for STABLE's expected flight performance.

2. RELEVANT PREVIOUS HAB MISSIONS

On the night of May 18th 1968, the STRATOSCOPE II launched and (to the authors' knowledge) attempted, for the first time in history, to achieve sub-arcsecond pointing of a balloon-borne observatory [2]. McCarthy describes the Stratoscope II hardware as 0.9 m (36-inch) L-shaped telescope with physical dimensions 4.9 m (16 ft) long, 7.6 m (25 ft) high, for a staggering ~3600 kg (8000 lbf) total mass. The system used guide stars in the visible spectrum with magnitudes between 5 and 7.5. Although STRATOSCOPE II was not designed to measure its pointing performance (instead, McCarthy et. al. estimated post-flight results by correlating data of the pointing servo, retrodivider, and microdensitometer scan of photographic images), the system was estimated to have achieved 0.02 arcseconds with the dimmest guide stars they used (the confidence level for these numbers are not clear from the text). Even with this remarkable achievement, McCarthy points out that "the flight environment is hostile" with its low temperature and large gradients induced on the optics. Another notable disturbance on the mission came from the high-frequency vibrations imparted by the platform itself. The inability to control high-frequency vibrations forced them to turn off most of their actuators while collecting the science images. Although this approach clearly worked for their very large system (with correspondingly favorable dynamics) at the dawn of the HAB fine pointing era, this

limitation revealed decades ago a fact that remains true today: high-bandwidth control is a critical element to advancing the pointing technology for HABs.

Since then, many other missions have targeted this type of performance in various contexts, for example, the SUNRISE [3], the WASP [4] and the BLAST missions [5]. The paragraphs below summarize the objective and performance of these missions.

The SUNRISE mission's objectives are to take high-resolution ultraviolet (UV) and visible observations of the sun from the stratosphere [3]. SUNRISE UV science requires a very small wavefront error; part of this error is controlled by the pointing stability performance. The SUNRISE gondola provides 7.5 arcsecond RMS pointing error while the CWS (Correlating Wave-Front Sensor) brings the error down to 0.05 arcseconds at the science instruments. The CWS uses a tip-tilt mirror as actuators and signal from the sun to drive it. The closed loop bandwidth is 70 Hz. SUNRISE is one of the few missions to create a high-bandwidth loop on an HAB capable of achieving this subarcsecond pointing for ultraviolet and visible observations. However, because its control system used the sun as a guide source, its direct application to non-solar astronomy are limited.

Another system that has achieved fine pointing is the Wallops Arc Second Pointer (WASP) System. WASP was developed at and is maintained by the Wallops Flight Facility (WFF). The history of its development is detailed by Stuchlik [4]. Its main objective is to provide a reusable balloon platform capable of pointing a science instrument with arcsecond accuracy and stability along two axes. WASP has completed multiple flights, both with and without a payload. It uses an LN-251 IMU, a sun and star camera, a reaction wheel, and gimbal motor drives to control the platform pointing stability to below one arcsecond. Performance varies with different payloads in different flights, but the most recent flight achieved 0.47 arcseconds RMS in pitch and 0.37 arcseconds RMS in yaw with a 0.5 m telescope as payload. This accomplishment marks an important milestone in HAB pointing technology. However, STABLE seeks to further mature this kind of technology by achieving a stability approximately a factor of four times better.

The STABLE system is the fine stage of the BIT-STABLE system and so relies on the performance of its outer stage (BIT) to achieve its final pointing performance. BIT is designed based on the gondola from the BLAST (Balloon-borne Large Aperture Submillimeter Telescope) mission. BLAST is a suborbital surveying experiment designed to study the evolutionary history and processes of star formation in local galaxies (including the Milky Way) and galaxies at cosmological distances [5]. The BLAST gondola provided better than 5 arcsecond pointing accuracy while scanning the sky. The pointing control was achieved with a coarse-fine stage pairing. Much like BIT,

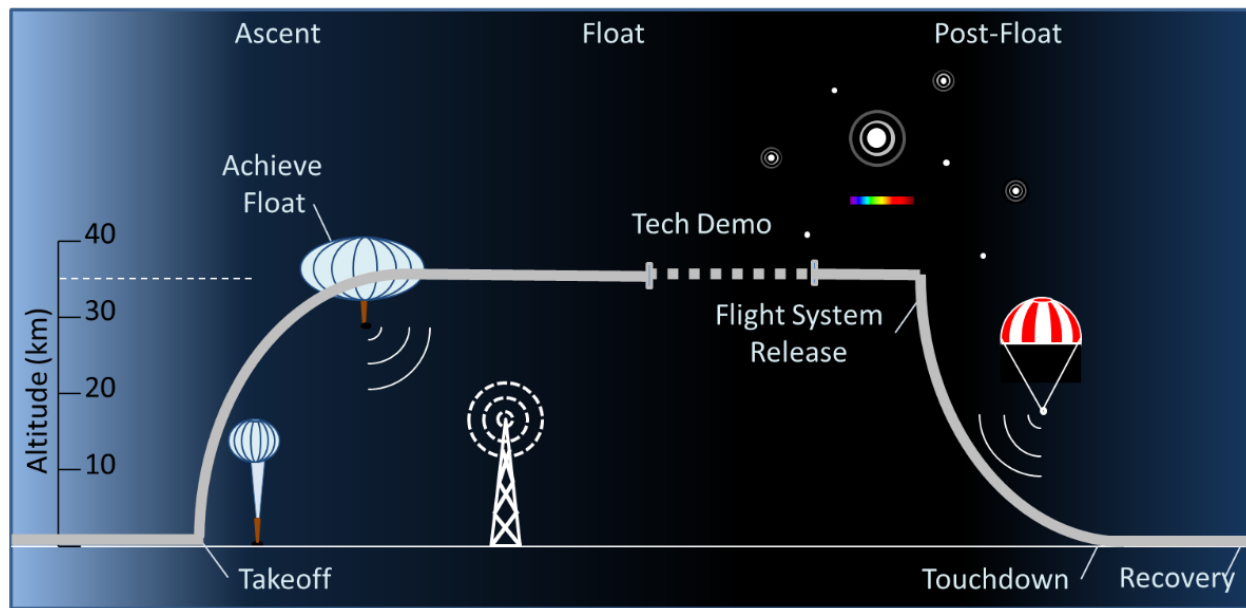


Figure 1 The BIT-STABLE mission concept of operations. Note that the time of day of the takeoff and touchdown varies by launch facility – this figure is not intended to suggest a particular launch site timeline.

the BLAST coarse stage used an elevation gimbal encoder, a tilt sensor, a sun sensor, a differential GPS unit, and a magnetometer. The pointing actuators were three torque motors: the reaction wheel, pivot, and elevation motors. BLAST used a fine stage with two CCD cameras and fiber optic gyroscope. In addition to informing the BIT gondola, the flight data and lessons learned from the BLAST mission proved to be the starting point for the design of the controller for the STABLE fine stage.

3. MISSION OVERVIEW

The BIT-STABLE mission system consists of a ground station and a flight system including the BIT gondola/coarse stage (designed and built by the University of Toronto), the STABLE payload/fine stage (designed and built at JPL with the guide camera characterized and provided by a UK consortium). Together, these stages not only rejected disturbances across the system, but were able to compensate for the rotation of the field of view over limited times, a capability not always found in other missions. BIT-STABLE also had an interface with the balloon launch vehicle and associated support equipment. The system was designed to be able to accommodate a variety of potential balloon providers to improve the chances that the system will fly.

In order to preserve this launch provider flexibility, the mission concept of operations and the environmental requirements on the system were selected to be the bounding cases across three potential launch locations: Kiruna, Sweden; Timmins, Ontario, Canada; and Fort Sumner, New Mexico, United States. STABLE was designed to support at most a 24 hour flight, including a nighttime technology demonstration phase of at least 8

hours long. As shown in Figure 1, STABLE's target altitude for observations is 35 km, although higher altitudes provide both better seeing and a more benign thermal environment. Altitudes between 30 km and 40 km were considered for the STABLE STOP (structural-thermal-optical performance) analysis that formed the basis for a large portion of the STABLE performance prediction. [6]

Once at float, the BIT outer stage points the STABLE telescope at a given target star. Target stars are pre-selected on the ground and uploaded to the BIT main computer in a sequence (although new sequences can be uploaded during the mission). The STABLE primary objectives require that it achieves its pointing performance with an SNR of 25 at the STABLE guide camera detector – which corresponds to a magnitude 10 star. STABLE also plans to observe a variety of stars to better characterize how pointing performance changes with different targets. The dimmest stars considered in the STABLE experiment plan are magnitude 14.

As soon as BIT has locked on to the attitude that places the stellar target on the STABLE detector, the gondola sends a signal to the STABLE main computer indicating the target of a given magnitude is available. The gondola then maintains its coarse pointing at that attitude until the observation ends. STABLE then enters a search sequence to find the star. If a target of the expected magnitude is not found on the detector, STABLE sends a "target not found" signal back to the gondola, which causes the gondola to adjust its pointing by a set amount and try again. If a target is found, STABLE initiates a fine refocus sequence that confirms the expected magnitude of the star, focuses the system to sharpen the point spread function, and generates an estimate of the static alignment error that is later used to

Table 1 STABLE driving environments. Environments deemed critical are found in dark blue, other environments considered in the design are found in light blue, and not applicable or benign environments are found in gray. Note that the transportation and launch environment did not drive the design.

Environment	Dynamics	Thermal	Pressure	EMI/EMC	Radiation	Humidity
Transportation/Ground	Shipping vibration levels, ~ 2.25g max	Less driving than float conditions	Standard atmosphere ~ 1 bar			Humidity-controlled vehicle
Launch	Initial balloon & payload release, ~ < 2g	Varies by launch site and season, but can be hottest ambient temp				Designed for 0-100% with some graceful performance degradation after 90%
Ascent		Convective effects dominate, Air temperature -67 C to -45 C	Designed to withstand depressurization, outgassing	Design to tolerate UHF transmissions found at launch site		
Float, During Non-Observational Periods		Air temperature -65 C to -38 C	Vacuum, 6-20 mbar		SEE tolerant design	
Float, During Observations	Vibration disturbance profile drives control loop design	Air temperature -65 C to -38 C				
Post Float	Cut down load, 10g					

adjust the coarse BIT pointing. The BIT-STABLE mission is a pointing stability demonstration, not a pointing accuracy or control demonstration, so these static errors are only documented to ensure that the target continues to remain on the detector. Once the fine focus sequence is complete, STABLE engages its control loop to achieve its fine pointing lock.

The STABLE requirements call for observations of at most 10 minutes for each stellar target to limit the amount of thermal drift and optical distortion that occurs over the course of one observation. The observation can end one of three ways: by losing the target out of the control window, by receiving a signal from the gondola to stop, or after holding the lock for a set period of time (nominally set to 10 minutes). Selected telemetry is sent back to the gondola for downlink during the mission, but the full suite of data are stored on a memory device in the STABLE payload for recovery after the mission.

Once the observation is complete, STABLE sends a message to the gondola indicating that the observation is complete. The gondola then points to the next target and repeats the sequence until the technology demonstration is over. Afterwards, the system is released from the balloon, a parachute is deployed, and the whole system is recovered by the launch facility.

4. THE BALLOON ENVIRONMENT AND ITS CHALLENGES

The HAB mission environment – and all of the environments the system experiences throughout its lifetime as a part of preparing for the launch – is fraught

with a set of unique challenges that set it apart from other platforms. The HAB float environment during the observation period was the focus of a significant amount of STABLE’s design effort. In particular, the thermal and vibration environments at float were the most challenging issues that had to be addressed in order to achieve the STABLE performance requirements.

As countless balloon flights have demonstrated, the thermally-induced environment acting on a HAB payload is complex. For optical systems, the thermal environment can induce aberrations and misalignments that affect both the guide system and any potential science instrument. These issues can be difficult to mitigate if they are not predicted and modeled appropriately. The ideal solution is to design an athermal optical train, but this kind of design can be expensive to implement. The STABLE team opted for a design that was only partially athermal and relied on conservative modeling assumptions. The thermal environment and modeling assumptions, as well as the mechanical and optical solutions and mitigations, are described in detail by Borden et. al. [6].

While the externally-induced vibration environment is fairly benign above the tropopause, a typical pointing system is equipped with notoriously noisy actuators such as motors and reaction wheels. The vibrations from these moving parts can and will affect the performance of a pointing system. Pointing from STRATOSCOPE II, SUNRISE, BLAST, and WASP have all been affected by this issue at some level. Because these vibrations have fairly high frequency content, a closed loop system with high bandwidth (~50Hz) is imperative to reach stability

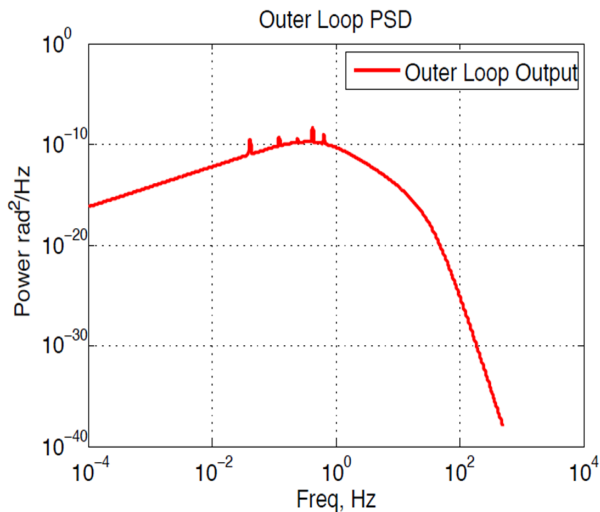


Figure 2 Required outer loop power spectral density function to limit the overall error contribution of the coarse pointing stage

performance well below 1 arcsecond. To complicate the problem, the majority of the vibration sources are in the coarse stage (BIT), which means the vibrations are part of the interface just like mass, and power, hence have to be allocated, agreed upon, and managed. In order to manage this part of the interface, the STABLE team imposed a requirement that the BIT gondola have a power spectral density below the line shown in Figure 2. In order to avoid being overly conservative, larger amplitudes are allowed at specific frequencies where BLAST saw increased power (because the BLAST gondola is the predecessor to the BIT gondola). This PSD corresponds to a total error of 2 arcseconds ($1\text{-}\sigma$) over 120 seconds.

Even though these thermal and vibration environmental issues were driving the quality of the observations and the pointing control and therefore the design of the system, the team also performed a thorough analysis of other environmental factors (see Table 1) to assess if they might in fact drive some of the design. STABLE had to be designed to operate even after exposure to the ground, launch, and ascent environments, and the launch facilities have rules regarding the system's structural integrity that are driven by the post-float (flight train cut-down, parachute deployment, descent, landing, and recovery) phases. Of particular note are the following:

1. As it is transported by truck to and from the launch and integration facilities, the system will be subject to vibration that can perturb its alignment. STABLE was designed to tolerate the mechanical loading of this transportation method as detailed in published standards, and the operations plan calls for re-aligning the optical system after every transport. After transport to the launch facility, all alignment degrees of freedom are fixed in place with epoxy.
2. During ascent, the pressure decreases dramatically from 1 bar to between 6 and 20 mbar at float. The

STABLE hardware contains no large sealed cavities that could cause a venting concerns due to this depressurization.

3. For HABs, the total radiation dose is not typically large, but several missions have experienced single event effects (SEEs) at these altitudes. STABLE sensors and flight computers are susceptible to SEEs but the software has been designed to mitigate the risk by tolerating resets.
4. The post-float environment primarily consists of the cut-down from the balloon and the subsequent landing on the surface. This environment drives the survival mechanical loading with a notable 10 g shock caused by the parachute deployment. Because STABLE is not required to operate after its technology demonstration, its only requirement against these mechanical loads are the need to maintain a positive margin with respect to ultimate yield to satisfy the launch facilities requirements that forbid the disintegration of the hardware.

5. STABLE DESIGN

The STABLE's as-built assembly, shown in Figure 3, has a total mass of 155.35 kg (not including the inner frame interface to the BIT gondola), and its total predicted power consumption is 152 W (average) or 700 W (peak). Over the 24 hour notional mission concept of operations, the predicted energy consumption of the STABLE system is 2747 W-hr. (Note that different launch sites have different total flight durations, but 24 hours represents the maximum total duration expected of the potential BIT-STABLE launch sites.)

The STABLE payload has two main subassemblies (see Figure 3): the telescope, which consists of the primary mirror, secondary mirror, and all of the supporting mechanical structure associated with them, and the Integrated Optical Bench Assembly (IOBA), which is the optical bench in the rear of the telescope and the mechanical platform where the remainder of STABLE's hardware is mounted.

The following section will briefly describe the design of each subsystem in the STABLE payload. The values discussed in this section are in part drawn from formal internal delivery documents and represent the best measured or analyzed values of the system from the STABLE integration and test period. Because STABLE has not yet flown, no flight values are available.

Telescope and Optical Train

The STABLE optical design is shown in Figure 4. The F/18, Ritchey-Chrétien telescope built by Equinox Interscience has the only optics with power in the system. The F/3 primary mirror is 0.5 m in diameter and made of Zerodur Class 0 with an aluminum coating. The secondary is a 12cm mirror made of Zerodur Class 0 with an aluminum coating. The secondary mirror can be adjusted

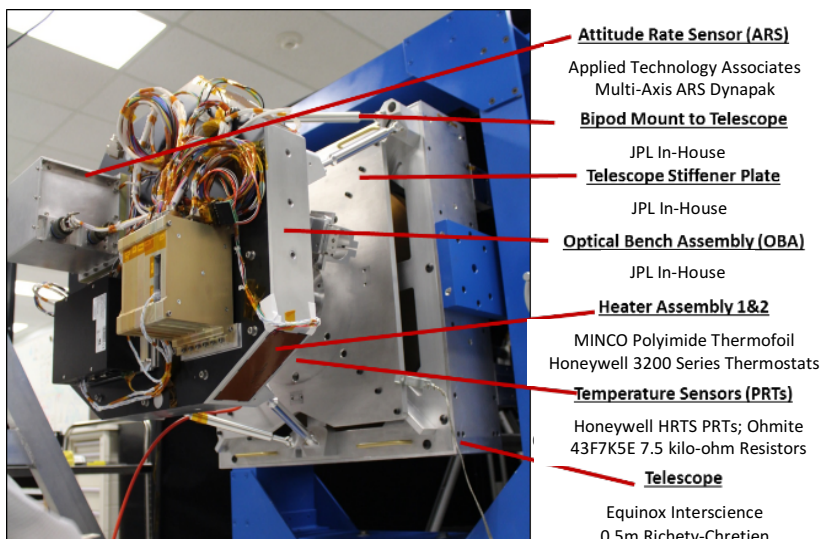
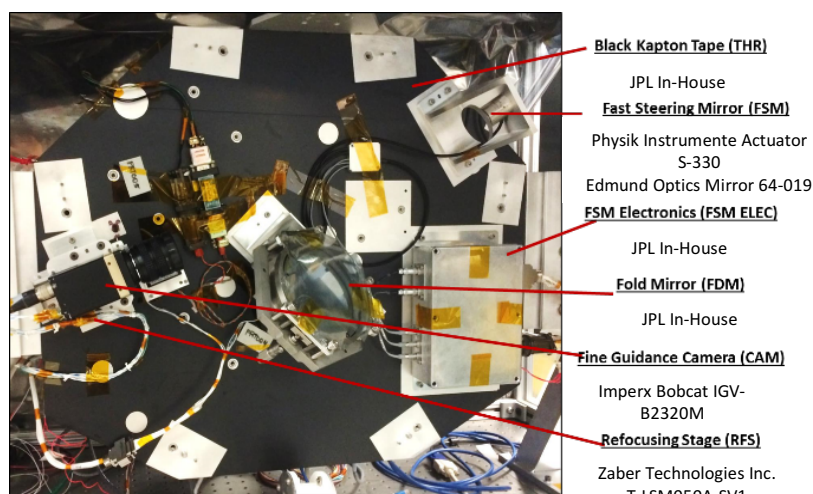
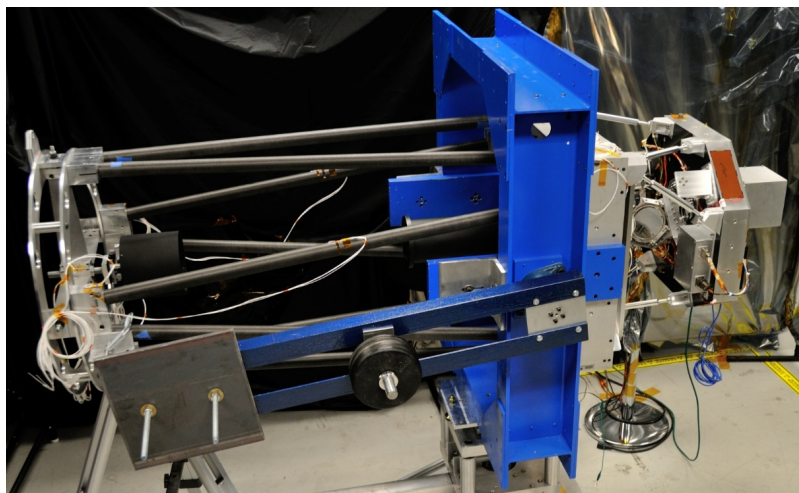


Figure 3 STABLE hardware components, including both sides of the Integrated Optical Bench Assembly

on the ground in tip, tilt, piston, and two-axis translation, but cannot be actuated during flight.

The next element in the optical path is the fold mirror. This flat mirror places the beam of light into the plane of the IOBA and can be adjusted on the ground in tip and tilt. The fast steering mirror (FSM) is the only actuated mirror during the flight. It can move in tip and tilt and is used to control the pointing stability of the point spread function on the guide detector. More information on the design of the optical system can be found in Borden, et. al. [6].

Control Loop Sensors

STABLE has two sensors that are used to achieve the desired stability: the fine guidance camera and the Attitude Rate Sensor (ARS).

The STABLE fine guidance camera is an off-the-shelf Imperx Bobcat IGV-B2320M, which has a CCD with microlenses in front of its $5.5 \mu\text{m}$ pixels (which are 0.13 arcseconds on the sky in the STABLE system). The unit has a detector of 2336×1752 pixels, which corresponds to 4.91 arcminutes \times 3.68 arcminutes on the sky and 12.85×9.64 mm in physical extent. The detector is sensitive in the visible wavelengths, with an absolute quantum efficiency shown in Figure 5. [7] The camera system is triggered by the STABLE control loop to collect images at 50 Hz. The STABLE flight camera performance was extensively characterized and described by Clark et. al [8].

The ARS is a high-performance three-axis Dynapak sensor from Applied Technology Associates that provides voltage measurements that can be interpreted into angular rate information, which is ultimately provided to the STABLE control loop. The sensor is sampled at 1 kHz to provide high-frequency relative corrections in between camera images in the control loop.

Control Loop Actuators

STABLE contains two actuators: the Fast Steering Mirror (FSM) and the Refocusing Stage (RFS).

The FSM has three components: a piezoelectric actuator, a mirror, and drive electronics. The piezoelectric actuator is a customized Physik Instrumente S-330 with a measured maximum stroke of ± 206 arcseconds. Strain gauges included in the

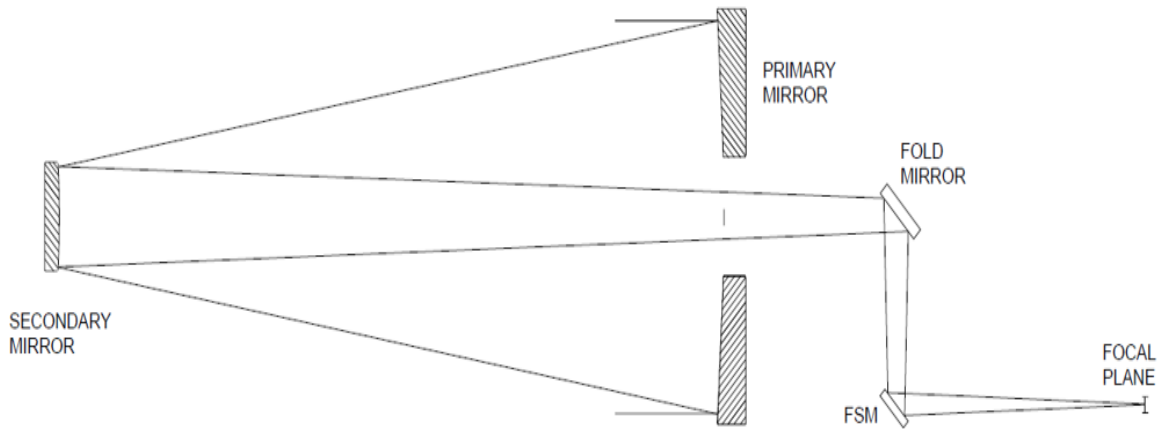
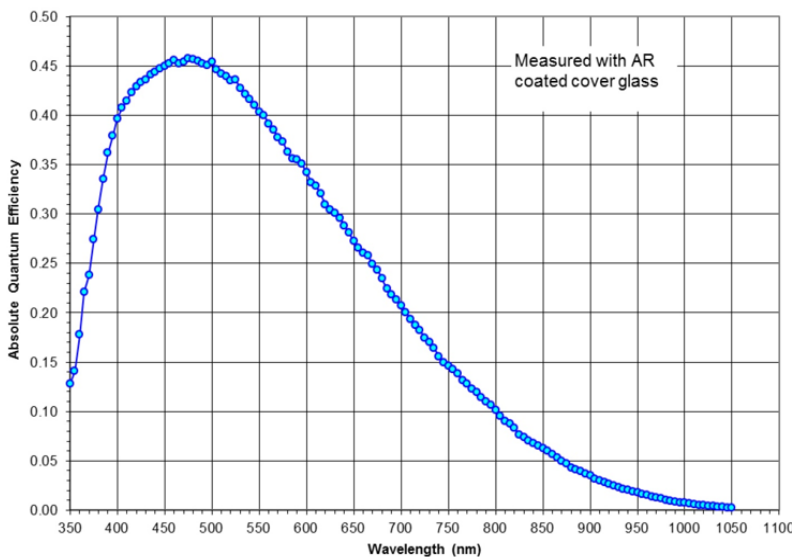


Figure 4 STABLE optical design

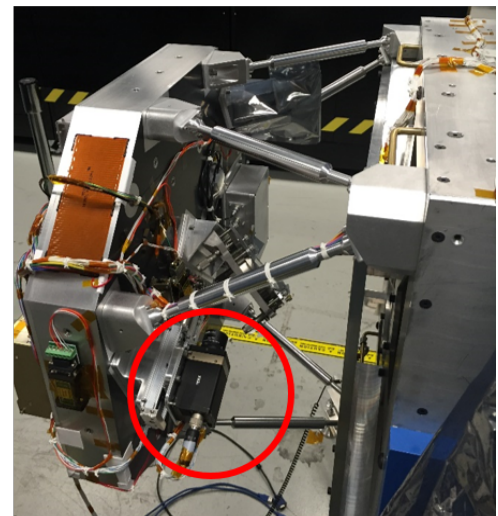
piezoelectric actuator packaging are included to determine the actuator position. Mounted on top of the piezo actuator, the FSM flat mirror has a diameter of 4.8 cm and is made of fused silica. The electronics are custom-designed by JPL to be able to operate in the HAB mission environment and can tolerate a piezoelectric slew rate of up to 66 mrad/s. The electronics also include an internal control loop (which can be turned off) using the strain gauge information to minimize nonlinearities such as creep and hysteresis. Overall, this FSM system is the only actuator in the high-bandwidth control loop and is given commands at 1 kHz. It is not momentum-compensated because subsequent analysis showed that this functionality was not needed.

The RFS, on the other hand, is used in between observations to refocus the system after experiencing thermal drift and is not included in the high-bandwidth

control loop. The RFS, which carries the guide camera, is an off-the-shelf unit manufactured by Zaber Technologies (T-LSM050A-SV1). It has a maximum travel from one end to the other of 50 mm, and it can traverse this distance in less than 30 seconds. The settling time of the detector after a change of RFS position was measured to be less than 0.5 seconds. Although this commercial-off-the-shelf (COTS) unit is not designed to operate in a HAB environment, component testing showed that it can achieve a commanded position to within 60 μm across its operating thermal range ($-25\text{ }^{\circ}\text{C}$ to $+30\text{ }^{\circ}\text{C}$) even under a worst-case inclination angle and a harness-induced resistive force of 1 N.



(a)



(b)

Figure 5 STABLE Camera (a) detector Quantum Efficiency, reproduced from the vendor-supplied specification sheet [7], (b) mounted on the integrated optical bench assembly

Thermal Hardware

The STABLE thermal system has different strategies for the two main hardware assemblies (the telescope and IOBA). The telescope temperature is not actively controlled, but eight Honeywell HRTS-5760-B-U Platinum Resistance Thermometers (PRT) are mounted on the thermally-sensitive elements on the telescope to measure the effect of the environment on the telescope temperature. [9] All PRT values are recorded in telemetry in order to estimate (on the ground) parameters such as the effective focal length. Thermal analyses for the system (described in more detail in Borden et. al. [6]) suggest that the telescope will remain below 0 °C even in the hottest bounding case.

For the IOBA, on the other hand, the thermal system is designed to maintain a temperature between 2 °C and 8 °C across the assembly using two thermostat-controlled heaters reading the temperature from two additional PRT sensors. These heaters make the STABLE thermal system the largest consumer of energy on STABLE. This temperature range was selected to lower the risk of performance degradation for the COTS parts mounted to the IOBA due to excessively cold temperatures. However, because of the low thermal conductivity through the carriage of the RFS, there were concerns that the guide camera was actually nearing its maximum allowable temperature during operation. To prevent this overheating, the camera is connected to the IOBA with a thermal strap.

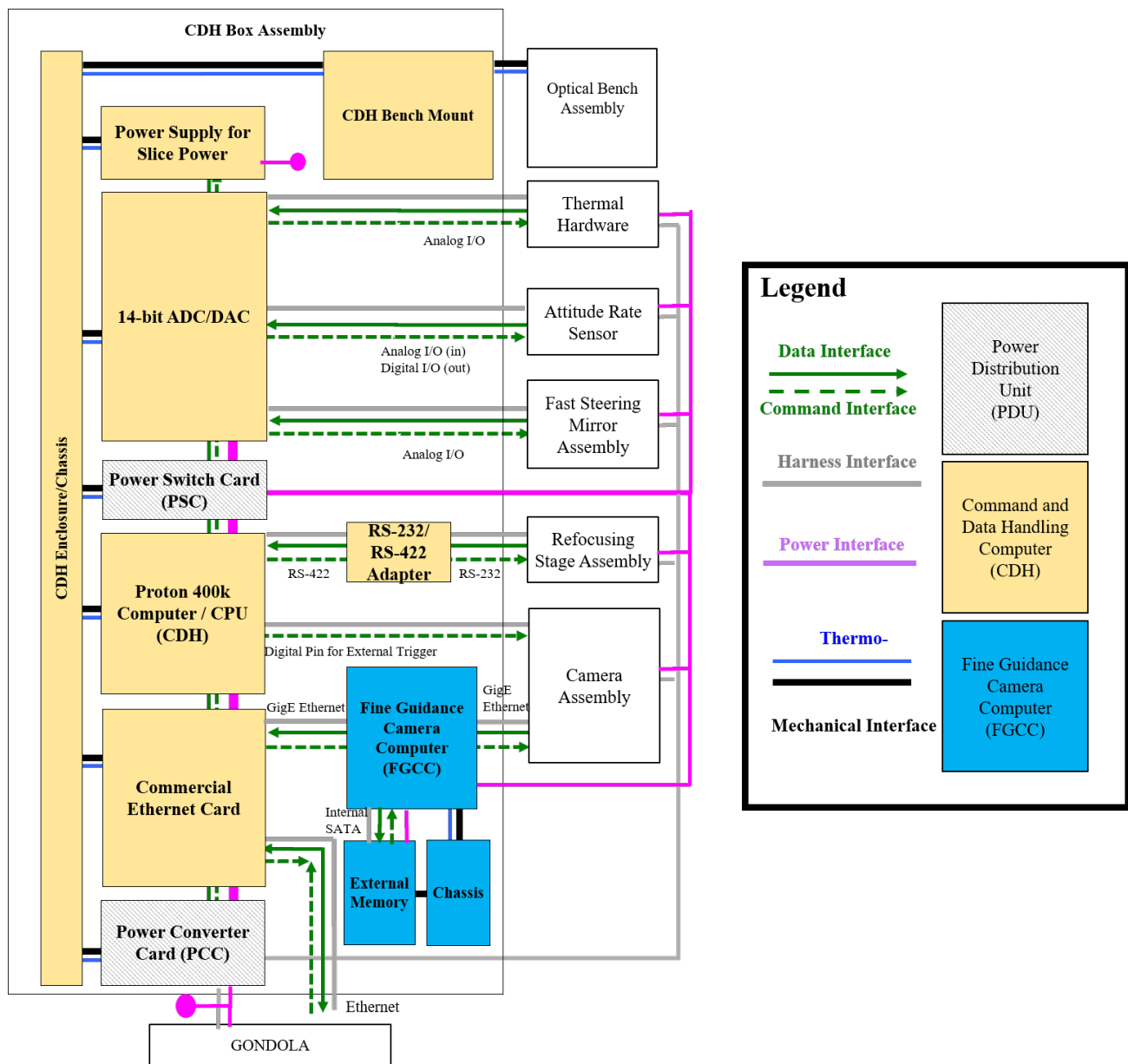


Figure 6 STABLE Avionics Block Diagram

The STABLE avionics system, shown in Figure 6, includes the power distribution unit (PDU), the STABLE main flight computer box (CDH), and the Fine Guidance Camera Computer (FGCC). The STABLE PDU is a set of two cards that are mounted inside the main CDH assembly. The JPL-designed Power Converter Card in the PDU simply accepts unregulated 28 V ($-8\text{ V} / +4\text{ V}$) input and distributes it to the following lines: $\pm 12\text{ V}$ at 1 A, $+12\text{ V}$ at 2A, $+15\text{ V}$ at 0.5 A, $+28\text{ V}$ at 2.5 A, and two $+28\text{ V}$ at 4.3 A. The Power Switch Card then adds switches to each line. As a whole, the PDU can tolerate a sustained peak power of 200 W (including the unregulated thermal power).

The STABLE CDH assembly is a customized stack containing a set of cards including: a Proton400k running VxWorks, an analog-to-digital (ADC) with 12 significant bits and a digital-to-analog (DAC) converter with 14 significant bits, a power card, and an Ethernet card, in addition to the aforementioned PDU cards. The computer in the CDH box serves as both the STABLE interface with the gondola through an Ethernet connection, and the location of the bulk of the fine control loop software. The ADC/DAC has 27 ADC channels and 4 DAC channels, through these channels it is connected to the ARS, the FSM electronics, and the thermal hardware. The CDH also communicates with the refocusing stage via a serial connection and converter.

The FGCC is an Advantech PCM-9363 running Linux that serves as the primary interface with the guide camera. As shown in Figure 6, the FGCC sends commands to and collects data from the guide camera, but the CDH computer sends the digital trigger to collect images at the command

of the control algorithm. The FGCC is used to acquire and process the images, although the non-deterministic timing of the Ethernet connection leads to occasional dropped images during closed-loop mode. The FGCC also houses the algorithms that compute the centroid location of the point spread function in each image. These data are then stored on a solid state drive with 120 GB of non-volatile memory and can read and write memory at 50 MB/s.

Flight Software and Control Loop Algorithm

STABLE's software is responsible for handling communication with the coarse stage, managing faults, and successfully implementing the various phases of the technology demonstration (calibrating the camera, acquiring the guide star, and refocusing the detector, as well as running the control loop). The STABLE flight software architecture is designed to be a real-time platform for executing the control algorithm at 1000 Hz, maintaining camera image transport delay below 30ms, and managing the behavior of the entire payload autonomously during flight to collect the necessary information from each sensor and properly update the actuators.

The STABLE control loop is shown in Figure 7. To achieve subarcsecond stability, it is necessary to maximize the closed loop bandwidth to attenuate environmental dynamics and HAB induced vibrations, especially those at higher frequencies ($\sim 50\text{Hz}$). Although the disturbance environment for HABs is naturally characterized by lower frequency content, a typical HAB coarse pointing stage must use actuators such as reaction wheels or motors to control the platform. These actuators can induce higher frequency vibrations that travel through the structure and

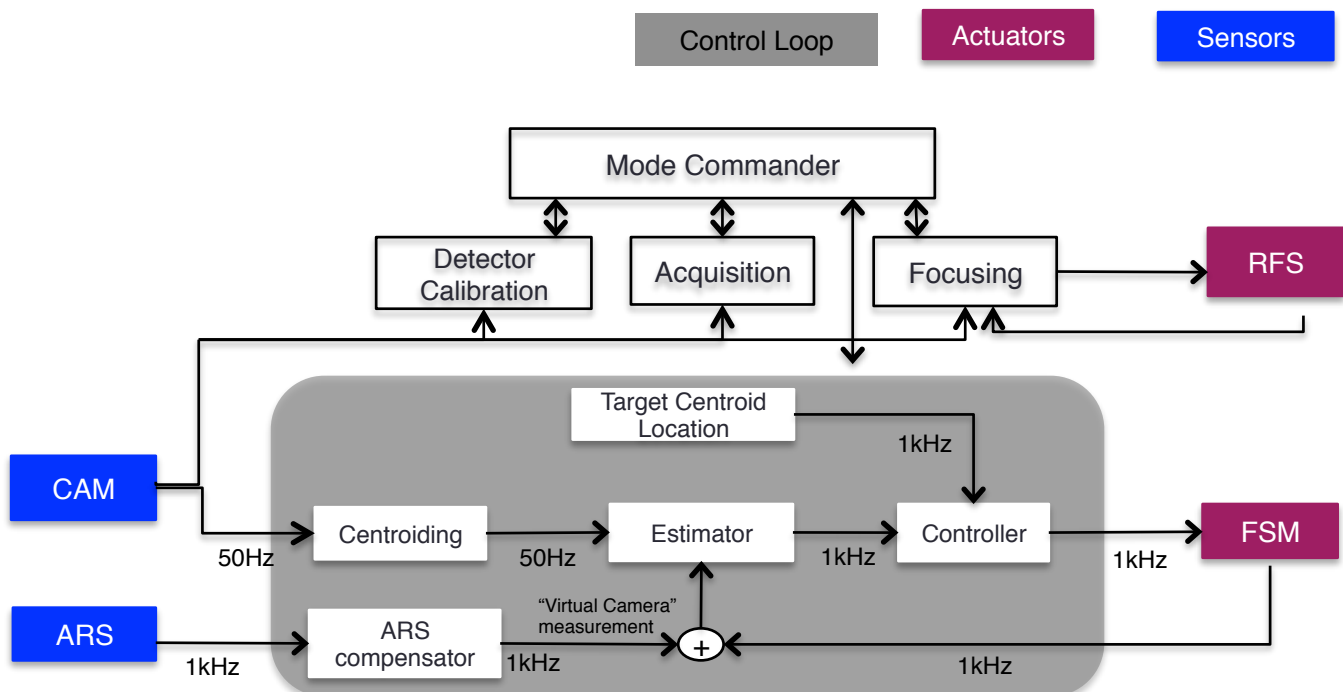


Figure 7 Control mode block diagram

cause unwanted motion of the line of sight (as experienced by WASP, SUNRISE, BLAST and expected by STRATOSCOPE II). After studying the disturbance environment and experiences of previous missions (specifically SUNRISE and BLAST), it was determined that 50 Hz control bandwidth was sufficient to achieve subarcsecond stability. STABLE's -3 dB bandwidth is thus approximately 65 Hz.

In order to achieve this bandwidth, the STABLE estimator algorithm blends 1 kHz information from the ARS and the FSM strain gauges, and 50 Hz information of the star centroid location on the camera detector to estimate the error of the line of sight with respect to a reference location. This information is then sent to the STABLE controller that provides commands to the FSM at 1 kHz. This blending of higher and lower frequency information is key to STABLE's control bandwidth. The ARS measurements can be used to estimate the angular rates at which the line of sight is moving but, if used as the sole feedback control sensor, would cause the line of sight to drift over time. The guidance camera provides direct line-of-sight absolute information that takes out the drift, but at lower frequency than the ARS can operate. In fact, in order to even support the 50 Hz image update, the STABLE centroiding algorithms use only a 100 x 100 pixel (0.21 arcminutes on the sky) window. This window is centered on the guide star's location on the detector at its first acquisition during that observation. The windowed image is stored for later analysis, but the entire image is not. This window size was chosen based on the assumed minimum coarse stage (BIT) 3σ stability performance, which corresponds to a motion of 47.5 pixel radius (6 arcseconds on the sky) over two minutes. Therefore, with this window size the point spread function of the guide star is likely to remain within the window so that STABLE can then control the stability of the system to within a 3σ motion of 2.4 pixels radius (0.3 arcseconds on the sky).

6. POINTING ERROR BUDGET

Given STABLE's design, it is clear that there are many factors in the system that can affect the pointing stability of the boresight of the telescope on the sky. These factors can be grouped together, as shown in the project error budget in Figure 8, into control errors and knowledge errors. Control errors come from the ability of the system to actively remove disturbances from the system dynamics given perfect knowledge, whereas knowledge errors affect the ability of the system to sense those disturbances. Note that not all errors are given separate allocations in the system error budget because they were instead controlled with detailed requirements specifying specific values for that parameter. Together, these errors must be below the required performance for STABLE's technology demonstration.

The STABLE allocations shown in Figure 8 highlight the fact that the majority of the pointing stability disturbances are expected to come from the pointing control errors. Control errors derive from the external and internal disturbances and their interactions with the flex body modes of the STABLE structure. The only STABLE-internal disturbance during an observation comes from the uncompensated actuated mass of the fast steering mirror. However, the anticipated interaction of this disturbance with the system's structural modes is small because the FSM actuated mass is small relative to the significant inertia of the IOBA. The interactions of the environmental disturbances with the STABLE structural modes are expected to be almost an order of magnitude larger than those due to the FSM motion. Similarly, certain mapping and alignment control errors can affect the control of the system, such as the mapping of the FSM motion onto the detector. The error budget required that the roll error (i.e., errors in the FSM tip/tilt motion that generated motion in the roll direction on the detector) be less than 2 mrad and the translational error (the error in the FSM range to the center of the detector due to imperfect control on the

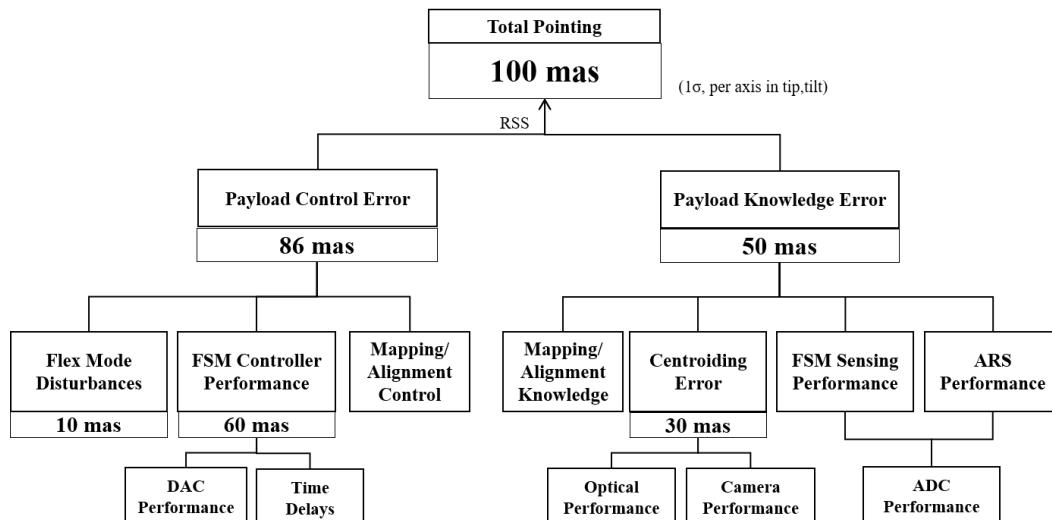


Figure 8 STABLE pointing error budget elements and selected allocations

translation stage) be less than 0.238 mm.

The largest element within the pointing error, however, is the transmission of environmental disturbances through the FSM controller. Although the gondola is designed to remove the bulk of these disturbances, the 2 arcseconds of remaining disturbance (in the profile shown in Figure 2) must be brought down by over an order of magnitude at the STABLE guide detector. A number of design elements influence this control performance, including the resolution and update frequency of the FSM actuator. Any disturbances above the STABLE bandwidth are passed through and contribute to this error, underscoring the importance of this value in the overall performance of the system.

The knowledge errors in the STABLE system are in many ways more complex than the control errors. The sensor performance, mapping and alignment errors, and centroiding errors all encompass many interrelated STABLE subsystems. For example, the performance of the ARS (angle random walk, rate random walk, scaling factors, etc.) and FSM strain gauges (scaling factors, etc.) clearly impact pointing knowledge. However, the effectiveness of the ADC used to read in the sensor data also plays a significant role in these errors. For example, when the ADC was discovered to have an effective number of bits of 12, rather than the 14 called for in the requirements, the system suffered an almost 20 milliarcsecond increase in its expected pointing error.

Similarly, the knowledge of the mapping of the FSM motion onto the detector and the mapping of the motion of the guide star onto the sky are incredibly important parameters for interpreting the pointing information that is collected. Parameters such as the effective focal length

(EFL) and the FSM ratio (the EFL divided by the distance of the FSM to the detector) capture these mappings, but because they are difficult to measure directly, the uncertainty in the parameters are related to the mechanical design, thermal drift, and dynamic motion of the various optical elements. Knowledge of the relative alignments of the system's sensors and actuators are similarly affected by these influences.

Another complex element in the pointing knowledge is the centroiding error. The optical system generates a point spread function of the target star on the guide detector, and the combination of the quality of that spot, the camera performance specifications, and the centroiding algorithm itself all contribute to the centroiding error. Because this part of the error budget encompasses a large portion of the STABLE system, it was tracked as a separate entity with its own allocation. The quality of the point spread function is largely influenced by the STABLE optical system behavior under the influence not only of the thermal environment but also of gravity. Heavy optical elements, such as STABLE primary mirror, are affected by their own weight as they are pointed at targets with different elevation angles. As the STABLE telescope is pointed at different stars during the mission, gravity causes mirror distortions (as well as structural distortions in the optical system), with larger distortions at higher elevation angles. In order to capture the range of potential environmental conditions that STABLE might experience, the team performed a full STOP (Structural-Thermal-Optical-Performance), as described by Borden et. al. [6]. The result of this STOP analysis was the optical performance over twelve thermal-gravity cases, described in Figure 9. The predicted shape of the point spread function can be generally characterized by a single number known as the Strehl ratio. A Strehl ratio of 0.8 or greater describes a

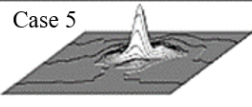
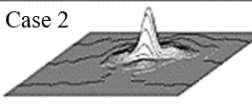
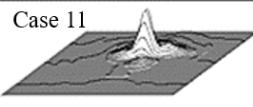
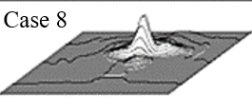
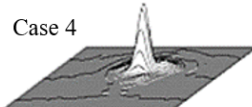
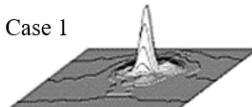
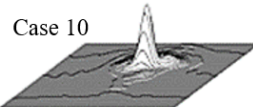
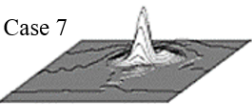
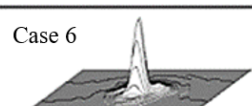
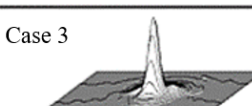
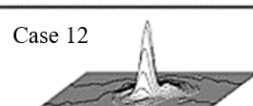

	Worst Case Hot	Nominal Beginning of Night	Nominal End of Night	Worst Case Cold
55° Elevation Angle	Case 5  SR = .492	Case 2  SR = .474	Case 11  SR = .444	Case 8  SR = .376
40° Elevation Angle	Case 4  SR = .650	Case 1  SR = .631	Case 10  SR = .573	Case 7  SR = .528
25° Elevation Angle	Case 6  SR = .739	Case 3  SR = .733	Case 12  SR = .694	Case 9  SR = .647

Figure 9 Point Spread Functions and Strehl ratios at various temperature and elevation angle scenarios (labeled as Case 1 to Case 12), as detailed in [6].

clear, diffraction-limited image, and lower numbers describe diffuse images with the photons spread over larger spot diameters. Although higher Strehl ratios are generally better for science, point spread functions with lower Strehl ratios may achieve better centroiding performance because the more diffuse image can provide a greater sensitivity to motion across pixels (up to a point). STABLE is designed to achieve a Strehl of 0.6 or better and does so in its nominal case, but the performance depends on the environmental conditions, so the pointing performance must be assessed over those different conditions as well.

7. STABLE PERFORMANCE

Although it has not yet been integrated into a gondola or flown on an HAB, STABLE's performance was estimated by an analysis of its pointing stability, and partially demonstrated in a controlled laboratory environment. The integration and test (I&T) period for the STABLE system was punctuated by extensive component performance testing, the results of which were used to run a set of end-to-end as-built analyses to estimate its ultimate performance. The I&T period culminated in a number of critical system-level tests, the most revealing of which are the ambient test and the stinger test. These tests directly probed elements of the STABLE performance and demonstrated a successful closed-loop system in a laboratory environment.

End-to-End Analysis

The end-to-end pointing stability analysis for STABLE was performed in the JPL-developed Control Analysis Simulation Testbed (CAST). CAST is a high-fidelity model of STABLE that incorporates the flexible body dynamics associated with the fast steering mirror and the structure as well as the as-built inputs from the hardware and configuration to determine the pointing stability of the system under different conditions. The main assumptions used in the end-to-end analysis – the factors from the STABLE error budget – are captured in Table 2. Most of these values come from component testing of the STABLE hardware or bounding estimates from individual analyses.

As shown in Table 3, the CAST analysis predicts that the pointing stability on flight during the nominal beginning of night, 40 degree elevation angle case (also shown in Figure 9) is 95 milliarcseconds (1- σ) or better, which meets the STABLE level-1 requirement to demonstrate pointing better than 100 milliarcseconds. Interestingly, the nominal case (case 1) produces the worst performance of the analyzed conditions, despite the Strehl ratio being much smaller for other conditions. This result suggests that a more diffuse (lower Strehl ratio) point spread function may slightly improve pointing performance. The analysis also shows that across the different STOP cases, the pointing performance does not vary by more than about 5 milliarcseconds, or 5% of the overall total. This result suggests that the STABLE system is well-designed and is robust to the variety of potential environmental conditions

it may experience in a HAB flight.

Table 2 Selected as-built parameters used in the end-to-end analysis of STABLE pointing performance.

Value	Axis	Measured/Best Known
Configuration		
Flex Body Dynamics		ON
ARS Compensator		ON
Star Magnitude		10
Flex Body Damping		0.05%
Mapping Errors		
Effective Focal Length (EFL) Knowledge Error		4.45 mm
FSM Ratio (EFL/Distance from FSM to Detector) Knowledge Error		21.391
FSM Roll Mapping Error		1.43 mrad
FSM Translational Mapping Error		0.196 mm
Alignment Errors		
ARS Alignment Error	x	0.4256 mrad
	y	0.3706 mrad
	z	1.6114 mrad
Camera Alignment Error	x	1.868 mrad
	y	17.261 mrad
	z	2.8798 mrad
FSM Alignment Error	x	0.7 mrad
	y	1.57 mrad
	z	23 mrad
Strain Gauge Alignment Error	x	0.7 mrad
	y	1.57 mrad
Scaling Errors		
ARS Scaling Error	x	1%
	y	1%
	z	1%
Strain Gauge Scaling Error	x	1%
	y	1%
Timing Errors/Delays		
Image Time Delay		25 ms
ARS Sensor Data Time Delay		1 ms
FSM Sensor Time Delay		1 ms
FSM Transport Delay		1 ms
DAC/ADC Issues		
DAC Quantization		14 bits
ADC Quantization		12 bits
DAC Noise		6 mV
Hardware Issues		
Dropped Camera Images		0.03%
Defocus Amount from RFS		0 mm
ARS Sensing Performance		
Angle Random Walk		1.25E-13 rad ² /s
Rate Random Walk		2.85E-11 rad ² /s ³

Table 3 STABLE pointing stability performance estimates over different STOP analysis conditions

STOP Analysis Conditions	Strehl Ratio of Point Spread Function	RMS 1- σ (mas)	
		Reference-Truth	
		Tip	Tilt
Case 1	0.631	94.5	89.4
Case 2	0.474	Not Performed	
Case 3	0.733	92.1	87.7
Case 4	0.65	90.9	86.2
Case 5	0.492	92.0	86.0
Case 6	0.739	93.7	89.2
Case 7	0.528	91.6	86.5
Case 8	0.376	93.8	84.0
Case 9	0.647	93.5	88.9
Case 10	0.573	92.6	87.4
Case 11	0.444	Not Performed	
Case 12	0.694	92.0	87.7

Laboratory Test

Although the end-to-end analysis provides evidence of the flight pointing performance of STABLE, it can only be truly tested under flight conditions. Thus, during the STABLE I&T, the team performed two tests (ambient and stinger) that exercised the camera-only portion of the control loop. The control loop was not using any information from the ARS in either test because its calibration could not be completed in the ground support fixtures available at the payload level. STABLE must be mated to its gondola before the ARS calibration can be completed. Without the ARS, the effective bandwidth of the STABLE controller is limited to that of the camera, which is significantly reduced from the required 50 Hz bandwidth that STABLE achieves when both sensors are active. These tabletop demonstrations had the IOBA secured to the top of a floating (actively correcting for disturbances from the lab floor) optical table, as shown in Figure 10, unattached to the telescope structure. The light source for the test was placed behind a set of optics that simulated the target star as seen through the telescope and cast onto the fold mirror.

The ambient test used a light source that was secured on the same table as the IOBA, and no disturbance was actively applied (the laboratory ambient environment provided the disturbance). If the control loop was turned off, the centroid of the simulated star (as computed by the centroid algorithm) wandered on the camera detector on both axes. As the control loop was turned on, the centroid position was kept within $\sim 0.5 \mu\text{m}$ ($1/10^{\text{th}}$ of a pixel), as shown in Figure 11.

In the stinger test, on the other hand, the light source was decoupled from the optical table and secured on a separate surface (a cement pillar designed to limit sensitivity to external disturbances). This configuration allowed the

team to excite the IOBA with an external disturbance source while the simulated star was fixed – a configuration analogous to flight. The IOBA was excited using a stinger which induced a force that did not pass through the center of mass, causing the IOBA to experience torques that generated a rocking motion along one of its axes. The stinger introduced a disturbance at 0.1 Hz, 0.25 Hz, and 1 Hz, which of course combines with the disturbance environment transmitted through the optical table to include some low-frequency drift. When the control loop was turned off, the centroid of the simulated star wandered on the camera detector, but when the control loop was turned on, the centroid position was kept within $\sim 2.5 \mu\text{m}$ ($1/2$ of a pixel). Figure 12 shows the performance data for the excitation at 0.25 Hz, which is typical of the other tests.

In both the ambient and stinger tests, the effect of the control loop is unmistakable. Even with a reduced bandwidth and limited control over the disturbance environment, the STABLE team was able to prove that the as-built closed loop system is effective at bringing down the errors in the pointing system, adding confidence to the end-to-end analysis that suggests that under flight conditions, this system will be able to meet its 100 milliarcsecond over 60 second pointing stability objective.

8. SUMMARY

In order for high altitude ballooning platforms to become a viable option for many astronomy and planetary science missions, they must first demonstrate fine pointing with guide targets that lend themselves to few operational and science target constraints. The BIT-STABLE mission is designed to demonstrate subarcsecond pointing using magnitude 10 stars in the visible spectrum from a HAB platform. The fine stage of this system, STABLE, in particular, is designed to take the 2 arcsecond residual error from the coarse stage (BIT) and bring it to 100

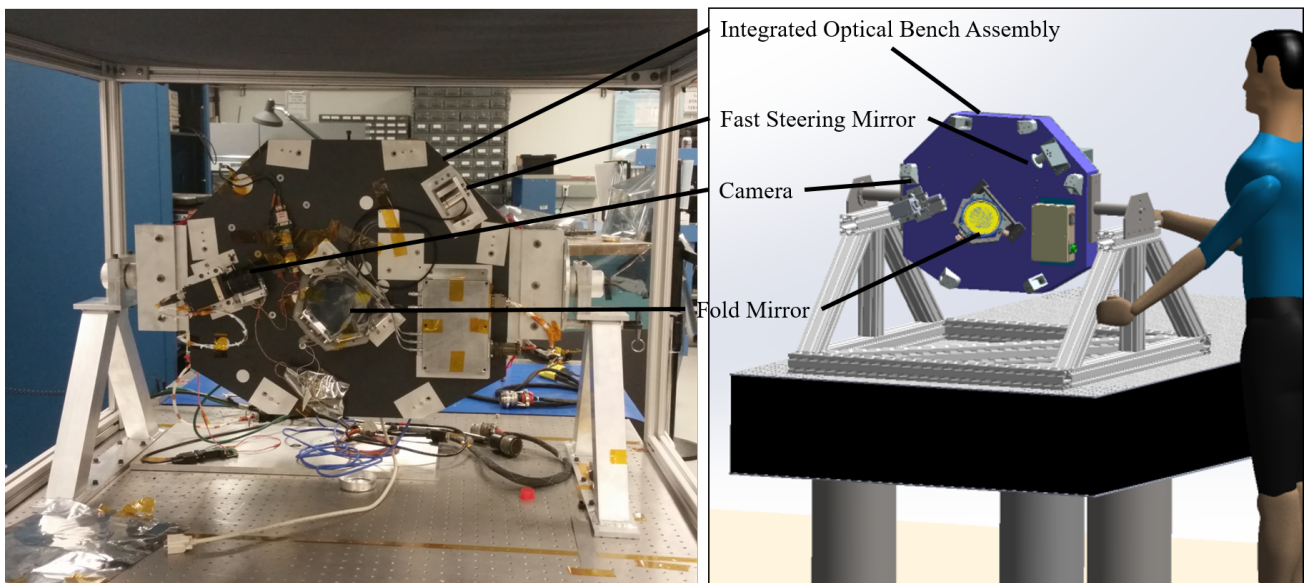


Figure 10 I&T setup for closed-loop testing

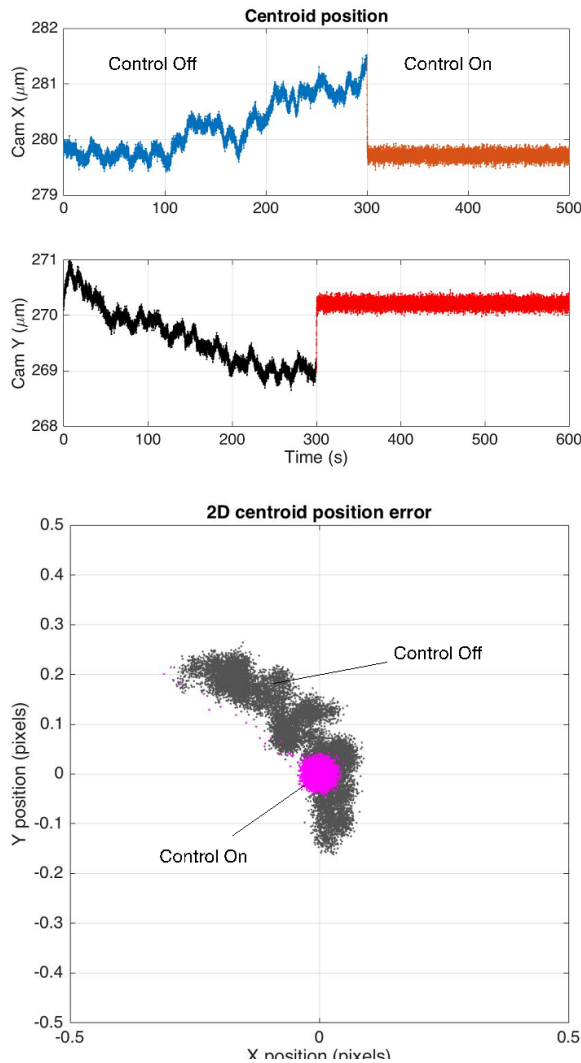


Figure 11 Experimental test results showing the closed loop performance under ambient conditions (sensing with 50 Hz camera images only)

milliarcsecond pointing stability over 60 seconds ($1-\sigma$). The system is designed to tolerate – and operate – in the demanding environments posed by a HAB platform, and the resulting design has been shown to meet its overall pointing objectives. Specifically, the end-to-end pointing performance estimates (which uses measured performance parameters from the as-built system) indicate that in a nominal thermal and gravity case, the system will achieve 94.5 milliarcseconds pointing stability over 60 seconds ($1-\sigma$). Additional tests in the laboratory environment demonstrate that the centroiding part of the control loop was successfully implemented in the STABLE hardware, buttressing the claims of the end-to-end system analysis. With these results, STABLE is well-poised to demonstrate this critical HAB platform technology in flight.

ACKNOWLEDGEMENTS

The research was carried out at the Jet Propulsion Laboratory, California Institute of Technology, under a contract with the National Aeronautics and Space

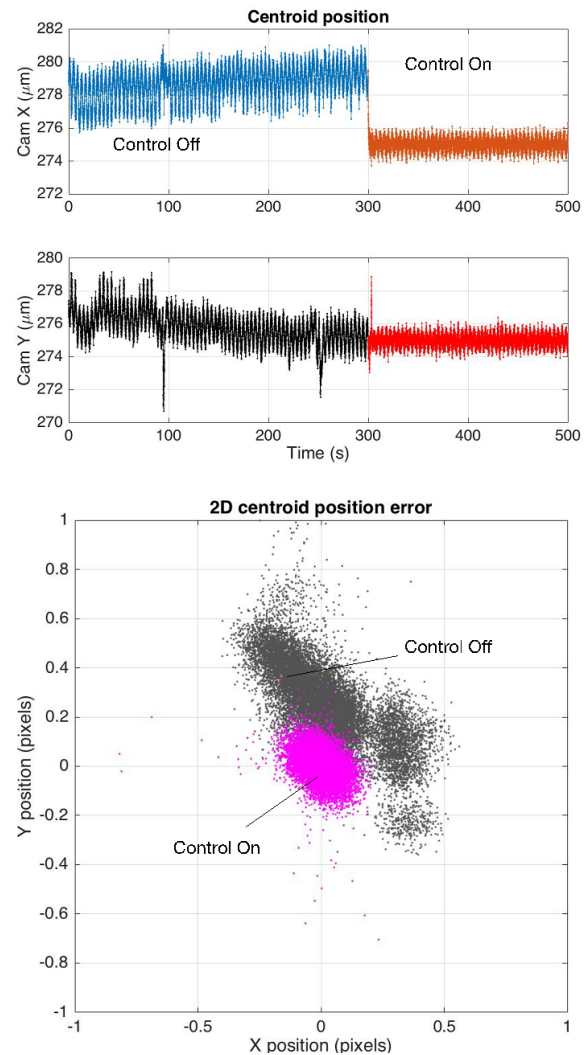


Figure 12 Experimental test results showing the closed loop performance with an external disturbance at 0.25 Hz using a stinger (sensing with 50 Hz camera images only)

Administration.

The authors would like to thank the remaining STABLE team members and contributors: Milan Mandic, Charlene Valerio, Clayton Williams as well as Chris Shelton, Anna Woodmansee, Grant Cavalier, John Maciejewski and the many others who were supportive of the STABLE project.

They thank Mark Balzer for his support in the JPL Mechanisms Lab during STABLE's integration and test.

They would also like to thank STABLE's formal mentors: Kim Aaron, David Bayard, Paul Brugarolas, David Durham, Renaud Goullioud, Yunjin Kim, Alan Lee, Christian Liebe, Stefan Martin, Jitendra Mehta, Zahidul Rahman, Eric Sunada, Bonnie Theberge, Marek Tuszynski, as well as the many other informal mentors who helped make this project a reality.

They would also like to thank BIT-STABLE partner Barth

Netterfield and the BIT team at the University of Toronto.

They would like to thank Jeff Booth, Jason Rhodes, and others for championing the project and Mike Sierchio and past program managers for providing guidance to the team.

REFERENCES

- [1] L. J. Romualdez, C. J. Damaren, L. Li, M. N. Galloway, J. W. Hartley, C. B. Netterfield, P. Clark and R. J. Massey, "Precise pointing and stabilization performance for the balloon-borne imaging testbed: 2015 test flight," *Proceedings of the Institution of Mechanical Engineers, Part G: Journal of Aerospace Engineering*, 18 May 2016.
- [2] D. McCarthy, "Operating Characteristics of the Stratoscope II Balloon-Borne Telescope," *IEEE Transactions on Aerospace and Electronic Systems*, vol. 5, no. 2, 1969.
- [3] P. Barthol et Al., "The Sunrise Mission," *Solar Physics*, vol. 268, pp. 1-34, 2011.
- [4] D. W. Stuchlik, "The Wallops Arc Second Pointer – A Balloon Borne Fine Pointing System," in *AIAA Balloon Systems Conference*, 2015.
- [5] E. Pascale et Al., "The balloon-borne large aperture submillimeter telescope: BLAST," *The Astrophysical Journal*, vol. 681, pp. 400-414, 2008.
- [6] M. Borden, D. Lewis, H. Ochoa, L. Jones-Wilson, S. Susca, M. Porter, R. Massey, P. Clark and B. Netterfield, "Thermal, Structural, and Optical Analysis of a Balloon-Based Imaging System," *Astronomical Society of the Pacific (Submitted for Publication)*.
- [7] Truesense Imaging, Inc., *KAI-04050 Image Sensor, 2336 (H) X 1752 (V) Interline CCD Image Sensor*, 2013.
- [8] P. Clark, R. Massey, H. Chang, M. Galloway, H. Israel, L. Jones, L. Li, M. Mandic, T. Morris, B. Netterfield, J. Peacock, R. Sharples and S. Susca, "Characterization of a commercial, front-illuminated interline transfer CCD camera for use as a guide camera on a balloon-borne telescope," *Journal of Astronomical Instrumentation*, vol. 3, p. 1440003, 2015.
- [9] H. Ochoa, *Thermal Control Design for the Subarcsecond Telescope and Balloon Experiment (STABLE)*, Cleveland, OH: NASA Glenn Research Center, 2014.

BIOGRAPHY



Laura Jones-Wilson earned her B.S. in Aerospace Engineering at Virginia Tech and went on to study at Cornell University, where she obtained her M.S. and Ph.D. in Aerospace Engineering, specializing in Dynamics and Controls. She then joined JPL in 2012 as a guidance and control systems engineer, where she served as the project systems engineer for STABLE until the project ended. She now serves as the PI of a Mars Sample Capture technology development effort, the co-manager of the SmallSat Dynamics Testbed, and the instrument engineer for Europa-UVS as a member of the Europa payload team.



Sara Susca received her PhD in Electrical Engineering from UCSB in 2007. She spent three years at Honeywell Aerospace developing new technology for GPS-denied navigation. She has been with JPL since 2011 where she covered various roles including Project Manager for STABLE (a balloon-borne sub-arcsecond pointing demonstration). She is currently member of the Europa Payload team as the instrument engineer for EIS and PIMS instruments.



Christina Diaz earned her B.S and M.S in Aerospace Engineering from the California Polytechnic State University, San Luis Obispo, specializing in astrodynamics and spacecraft design. She joined JPL in 2013 as a systems engineer participating in various roles from mission assurance for balloon-borne instruments and CubeSats to meteoroid/orbital debris and radiation environment definition. She is currently a member of the Mars2020 Payload team as the instrument engineer for the RIMFAX and MEDA science investigations.